

## ***Electronic Supplementary Information***

# **Photochemical Preparation of Gold Nanoparticle Decorated Cyclodextrin Vesicles with Tailored Plasmonic Properties**

*Wilke C. de Vries,<sup>†</sup> Maximilian Niehues,<sup>†</sup> Maren Wissing,<sup>†</sup> Thomas Würthwein,<sup>‡</sup> Florian  
Mäsing,<sup>†</sup> Carsten Fallnich,<sup>‡</sup> Armido Studer<sup>†</sup>, Bart Jan Ravoo<sup>\*†</sup>*

<sup>†</sup>Organic Chemistry Institute and Center for Soft Nanoscience, Westfälische Wilhelms-  
Universität Münster, Corrensstr. 40, D-48149 Münster, Germany.

<sup>‡</sup>Institute of Applied Physics, Westfälische Wilhelms-Universität Münster, Corrensstr. 2, D-  
48149 Münster, Germany.

Email: [b.j.ravoo@uni-muenster.de](mailto:b.j.ravoo@uni-muenster.de), [studer@uni-muenster.de](mailto:studer@uni-muenster.de)

## General

All reactions were carried out in heat-gun-dried glassware under argon atmosphere and were performed by using standard *Schlenk* techniques. Thin layer chromatography was carried out on *Merck* silica gel 60 F254 plates; detection by UV or dipping into a solution of  $\text{KMnO}_4$  (1.5 g),  $\text{NaHCO}_3$  (5.0 g) in  $\text{H}_2\text{O}$  (400 mL) followed by heating. Flash chromatography (FC) was carried out on *Merck* silica gel 60 (40 – 63  $\mu\text{m}$ ) at an argon pressure of 0-0.5 bar.

## Instrumentation

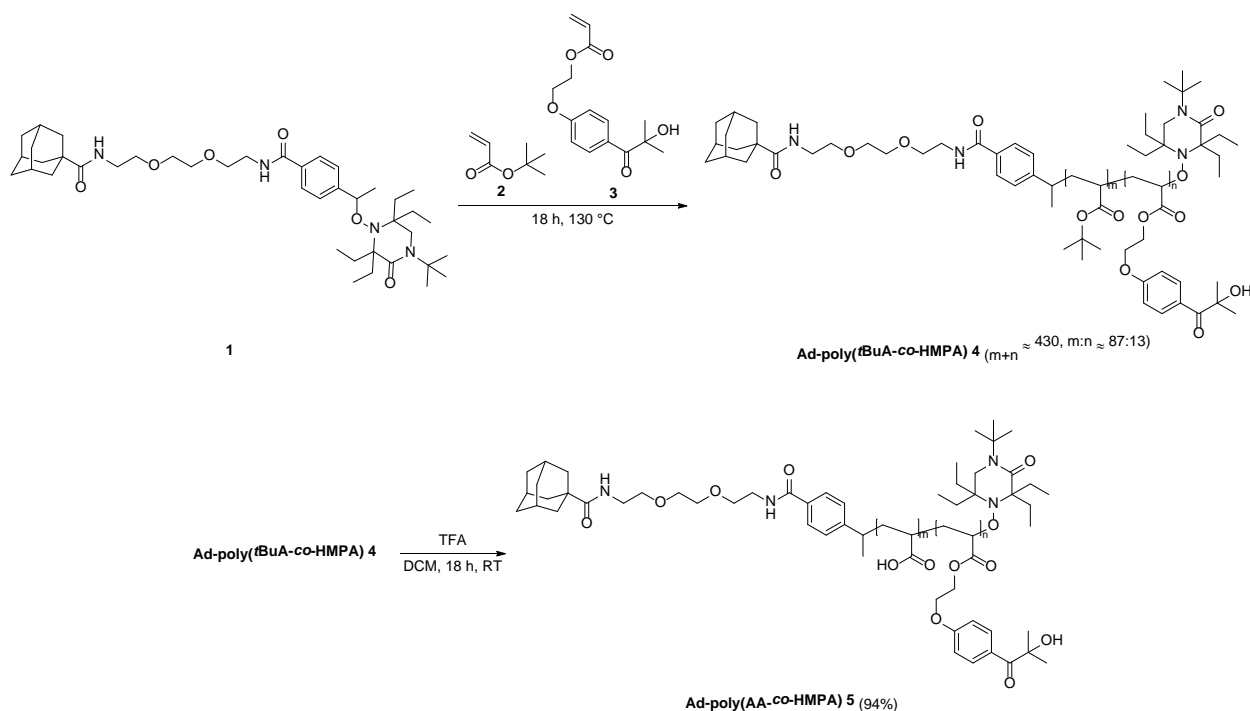
**$^1\text{H-NMR}$  and  $^{13}\text{C-NMR}$  spectra** were recorded on an *DPX 300* (Bruker), *Avance II 300* (Bruker), *Avance II 400* (Bruker) or a *DD2 600* (Agilent). Chemical shifts  $\delta$  in ppm are referenced to the solvent residual peak. **IR spectra** were recorded on a Digilab FTS 3100 FT-IR (Varian) equipped with a Specac MKII Golden Gate Single Reflection ATR unit (Varian). Signals were given in wavenumbers  $\nu$  ( $\text{cm}^{-1}$ ). Intensities were abbreviated with *s* (strong), *m* (medium), *w* (weak) and *br* (broad). **HRMS (ESI)** was performed using a MicroTOF ESI (Bruker) and an Orbitrap LTQ XL (Thermo Scientific). **Gel Permeation Chromatography (GPC)** was carried out with extra pure THF as eluent at a flow rate of  $1.0 \text{ mL min}^{-1}$  at  $25 \text{ }^\circ\text{C}$  on a system consisting a PSS SEcURITY GPC System (Polymer Standards Service), a set of two PLgel 5  $\mu\text{m}$  MIXED-C columns ( $300 \times 7.5 \text{ mm}$ , Agilent Technologies) plus a guard column. Data was analyzed with PSS WinGPC Compact software (version.7.20, Polymer Standards Service) based upon calibration curves built upon poly(methylmethacrylate) standards (Varian) with peak molecular weights ranging from 1660 to  $1000000 \text{ g mol}^{-1}$ . **Photoreactions** were performed in quartz glass tubes and initiated using a RPR-100 photochemical reactor (Southern New England Ultraviolet) equipped with 16 RPR-3500 UVA-lamps ( $\lambda_{\text{max}} = 350 \text{ nm}$ , Southern New England Ultraviolet). **Dynamic light scattering (DLS) and  $\zeta$ -potential** measurements were carried out on a Nano ZS Zetasizer (Malvern Instruments) at  $25 \text{ }^\circ\text{C}$  and samples were prepared in disposable 1 mL semi-micro PMMA cuvettes (BRAND) or in disposable DTS 1060 capillary cells (Malvern Instruments). Data analysis was performed with Zetasizer Software Version 7.12 (Malvern Instruments) and OriginPro 9.6 (Origin). **Transmission electron microscopy (TEM) and scanning transmission electron microscopy with high-angle annular dark-field detector (STEM-HAADF)** was performed using a Titan Themis G3 300 TEM (FEI) operating at 300 kV. The STEM elemental analysis was performed by using a quadrupole EDX detector. Sample preparation was performed by incubation of a glow-discharged carbon coated copper grid (S162, Plano) with 5  $\mu\text{L}$  of the sample for 1 min and gentle blotting with filter paper. To remove not immobilized particles and inorganic salts 10  $\mu\text{L}$  of ultrapure water were added and after 30 s gently blotted with filter paper. The sample was stained with 5  $\mu\text{L}$  of 0.5% (w/w) aqueous phosphotungstic acid (PTA) for 30 s and again gently blotted with filter paper. TEM measurement data was analyzed with Velox (version 2.3, Thermo Scientific) and ImageJ version 1.52h (National Institutes of Health, USA, Java 1.8.0\_66). **UV/vis absorption measurements** were performed with a V-770 double beam spectrophotometer (JASCO) at  $25 \text{ }^\circ\text{C}$ . Samples for spectroscopic measurements were prepared in disposable 1 mL semi-micro PMMA cuvettes (BRAND) and data analysis was done with Spectra Manager Version

2.14.06 (JASCO) and OriginPro 9.6 (Origin). **X-ray Photoelectron Spectroscopy (XPS)** was done with a Kratos Axis Ultra (Kratos) using a monochromated Al K $\alpha$  irradiation with an excitation energy of 1486.6 eV. For region scans a pass energy of 0.02 eV was employed. Data was analyzed with CasaXPS Software Suite (version 2.3.15). All spectra were calibrated to the binding energy of the C-1s-orbital in aliphatic carbon (285 eV). **Spontaneous Raman scattering spectra** were measured with a custom-built micro-spectrometer setup (Figure S16). As a light source, a continuous-wave diode-pumped solid-state laser at a wavelength of 640 nm was used (colored red in Figure S16). In order to adjust the laser power, the beam was transmitted through a rotatable half-wave plate and a polarizing beam splitter (not shown). The alignment of the linear polarization of the laser light could be adjusted by another half-wave plate (also not shown). The laser beam was expanded by a telescope setup consisting of two lenses (L) to a diameter of 2.0 mm (full width at half maximum) and directed into a 100 oil immersion microscope objective (MO) (numerical aperture of 1.3) focusing the beam into the sample in an inverted microscope geometry. These focusing parameters led to an estimated focus size of approximately 0.75  $\mu\text{m}$  (Gaussian beam width) with a Rayleigh length of 2.8  $\mu\text{m}$ . The sample was contained in a glass imaging chamber above the MO on a piezoelectric scanning table to enable nanometer precise positioning for the spectroscopic detection. The Raman scattered light (colored blue in Figure S16) was collected in backwards direction by the MO and transmitted through a dichroic mirror (DM) and focused by another lens onto the slit of a Czerny–Turner spectrograph using a charge-coupled device camera (CCD, AndorNewton 970) for the detection in the wavenumber region between 500 and 3300  $\text{cm}^{-1}$  with a resolution of 12  $\text{cm}^{-1}$ . Raman spectra were processed using Matlab (MathWorks) and OriginPro 9.6 (Origin) and background from Au@PSV and residual fluorescence of rhodamine was subtracted. **Ultrapure water** was generated with a PureLab UHQ (ELGA LabWater) water purification system. **Measurement of pH** was carried out using a SevenEasy<sup>TM</sup> pH meter with an InLab 413 electrode (Mettler Toledo). A three-point calibration with commercially available buffer standards (pH 4.01, 7.00, 9.21) was performed before each measurement.

## Materials

All chemicals were purchased from *Sigma Aldrich*, *Acros Organics*, *Merck*, *VWR* or *TCI* and used as received unless otherwise stated. Adamantyl-initiator **1**<sup>1</sup>, 2-(4-(2-hydroxy-2-methylpropanoyl)phenoxy)ethyl acrylate **3**<sup>2</sup>, amphiphilic  $\beta$ -cyclodextrin<sup>3,4</sup> and rhodamine adamantane conjugate (Ad-RhoB)<sup>5</sup> were prepared according to previously reported literature procedures. Phosphate buffered saline (PBS, 2 mM NaH<sub>2</sub>PO<sub>4</sub>, 18 mM Na<sub>2</sub>HPO<sub>4</sub>, 150 mM NaCl (all *Sigma Aldrich*), pH 7.4) was prepared using ultrapure water with a resistance higher than 18 M $\Omega$ .

## Synthesis



**Scheme S1.** Synthesis of Ad-poly(AA-co-HMPA) **5** starting from adamantyl-initiator **1**<sup>1</sup>, 2-(4-(2-hydroxy-2-methylpropanoyl)phenoxy)ethyl acrylate **3**<sup>2</sup> and *tert*-butyl acrylate **2**.

### Adamantyl terminated poly(*tert*-butylacrylate-*co*-2-(4-(2-hydroxy-2-methylpropanoyl)phenoxy)ethylacrylate) (Ad-poly(*t*BuA-*co*-HMPA) **4**)

According to a modified literature procedure by *Ravoo et al.*,<sup>1</sup> a heat gun-dried Schlenk tube was charged with adamantyl-initiator **1** (6.0 mg, 8.3 μmol, 1.0 eq.), 2-(4-(2-Hydroxy-2-methylpropanoyl)phenoxy)ethyl acrylate **3** (115 mg, 0.41 mmol, 50 eq.) and *tert*-butyl acrylate **2** (0.61 mL, 4.1 mmol, 500 eq.) under argon. The solution was degassed by conducting three freeze-thaw cycles. After the mixture was brought to rt the tube was sealed and the polymerization was carried out at 130 °C for 18 h. The reaction was cooled to rt and transferred to a round bottom flask using DCM. Solvents and residual *tert*-butyl acrylate were removed under reduced pressure. To remove residual 2-(4-(2-Hydroxy-2-methylpropanoyl)phenoxy)ethyl acrylate the polymer was dissolved in DCM (some drops) and precipitated with pentane (10 mL). The supernatant was decanted, and solvents were removed under reduced pressure. This dissolving-precipitation-cycle was carried out five times. Then the polymer was dried in vacuo. Conversion was determined gravimetrically. Molecular weight and PDI were determined by GPC at 25 °C against PMMA standards using THF as eluent. The title polymer **4** was obtained as a white solid (323 mg, 50%,  $M_n$ : 64 kDa, PDI: 1.4). The *tert*-butyl acrylate : 2-(4-(2-Hydroxy-2-methylpropanoyl)phenoxy)ethyl acrylate) – ratio was determined by <sup>1</sup>H NMR (*t*BuA : HMPA = 87 : 13).

**<sup>1</sup>H-NMR** (300 MHz, CDCl<sub>3</sub>, 298K):  $\delta$  = 8.12 – 8.00 (*br*, 2H, CH<sub>ar</sub>), 7.02 – 6.86 (*br*, 2H, CH<sub>ar</sub>), 4.55 – 4.07 (*br*, 5H, OCH<sub>2</sub>CH<sub>2</sub>O, OH), 2.42 (*br*, 1H, CH), 2.22 (*br*, ca. 7.5 H, CH), 1.90 – 1.31 (*br*, ca. 92 H, CH<sub>2</sub>, CH<sub>3</sub>) ppm.

**IR** (ATR):  $\nu$  = 2979<sub>w</sub>, 2935<sub>w</sub>, 2163<sub>w</sub>, 1726<sub>s</sub>, 1672<sub>w</sub>, 1602<sub>m</sub>, 1508<sub>w</sub>, 1480<sub>w</sub>, 1454<sub>w</sub>, 1393<sub>w</sub>, 1367<sub>m</sub>, 1254<sub>m</sub>, 1148<sub>s</sub>, 960<sub>w</sub>, 918<sub>w</sub>, 845<sub>m</sub>, 732<sub>m</sub>, 649<sub>w</sub> cm<sup>-1</sup>.

#### **Adamantyl terminated poly(acrylic acid-co-2-(4-(2-Hydroxy-2-methylpropanoyl) phenoxy) ethyl acrylate) (Ad-poly(AA-co-HMPA))**

The synthesis was performed following a modified literature procedure.<sup>1</sup> To a solution of Ad-poly(*t*BuA-co-HMPA) **4** (272 mg, 4.25  $\mu$ mol, app. 2.11 mmol of *tert*-butyl acrylate units, 1.00 eq.) in dry DCM (15 mL) trifluoroacetic acid (1.70 mL, 2.50 mg, 21.1 mmol, 10.0 eq.) was added slowly. The reaction mixture was stirred at rt for 18 h forming a white precipitate. The solvent was removed under reduced pressure and the polymer was dissolved in ultrapure water while the pH was adjusted to pH 7 by addition of 1 M NaOH. Dialysis (Spectra/Por 7 regenerated cellulose dialysis membranes, MWCO 6–8 kDa) against ultrapure water (3  $\times$  exchange of water in 24 h) and freeze-drying gave Ad-poly(AA-co-HMPA) **5** as a cottony white solid (173 mg, 4.01  $\mu$ mol, 94%).

**<sup>1</sup>H-NMR** (300 MHz, CDCl<sub>3</sub>, 298K):  $\delta$  = 8.07 (*br*, 2H, CH<sub>ar</sub>), 6.99 (*br*, 2H, CH<sub>ar</sub>), 4.71 – 3.88 (*br*, 4H, OCH<sub>2</sub>CH<sub>2</sub>O), 2.80 – 1.00 (*br*, ca. 32 H, CH, CH<sub>2</sub>, CH<sub>3</sub>) ppm.

**IR** (ATR):  $\nu$  = 3374<sub>br</sub>, 2940<sub>br</sub>, 1713<sub>m</sub>, 1667<sub>m</sub>, 1565<sub>s</sub>, 1453<sub>m</sub>, 1407<sub>s</sub>, 1256<sub>m</sub>, 1163<sub>s</sub>, 1061<sub>w</sub>, 960<sub>w</sub>, 842<sub>m</sub>, 767<sub>w</sub> cm<sup>-1</sup>.

#### **4-(2-hydroxyethoxy)benzoic acid**

The synthesis was performed following a modified literature procedure.<sup>6</sup> To a mixture of *para*-hydroxybenzoic acid (6.90 g, 50.0 mmol, 1.00 eq.), KOH (7.00 g, 125 mmol, 2.50 eq.), KI (2.90 g, 17.4 mmol, 0.35 eq.) in water (50 mL) 2-bromoethanol (7.50 g, 60.0 mmol, 1.20 eq.) was added slowly and the reaction mixture was refluxed for 18 h. After cooling to rt HCl (app. 12 M) was added dropwise until a white precipitate was formed. Upon filtration the white solid was recrystallized from ethanol twice giving 4-(2-hydroxyethoxy)benzoic acid as a crystalline white solid (6.57 g, 36.1 mmol, 72%).

**<sup>1</sup>H-NMR** (400 MHz, D<sub>2</sub>O, 298K):  $\delta$  = 8.00 (*m*, 2H, CH<sub>ar</sub>), 7.09 (*m*, 2H, CH<sub>ar</sub>), 4.22 (*t*, 2H, CH<sub>2</sub>), 3.95 (*t*, 2 H, CH<sub>2</sub>) ppm.

**<sup>13</sup>C-NMR** (100 MHz, MeOD, 298K):  $\delta$  = 169.8 (CO), 164.3 (C<sub>ar</sub>O), 132.8 (CH<sub>ar</sub>), 124.1 (C<sub>ar</sub>), 115.2 (CH<sub>ar</sub>), 70.8 (CH<sub>2</sub>), 61.5 (CH<sub>2</sub>) ppm.

**HRMS** (ESI):  $m/z$  = 205.0471 calculated for C<sub>9</sub>H<sub>10</sub>O<sub>4</sub>Na<sup>+</sup> ([M+Na]<sup>+</sup>), found: 205.0478.

**IR** (ATR):  $\nu$  = 3300<sub>br</sub>, 2952<sub>m</sub>, 2903<sub>m</sub>, 2863<sub>m</sub>, 2543<sub>br</sub>, 1672<sub>s</sub>, 1604<sub>s</sub>, 1580<sub>m</sub>, 1512<sub>m</sub>, 1459<sub>w</sub>, 1427<sub>s</sub>, 1320<sub>m</sub>, 1288<sub>m</sub>, 1250<sub>s</sub>, 1170<sub>s</sub>, 1130<sub>w</sub>, 1082<sub>s</sub>, 1043<sub>s</sub>, 962<sub>m</sub>, 946<sub>m</sub>, 892<sub>m</sub>, 847<sub>s</sub>, 822<sub>w</sub>, 769<sub>s</sub>, 694<sub>m</sub>, 644<sub>s</sub>, 627<sub>m</sub> cm<sup>-1</sup>.

## Additional Experimental Data

**Table S1.** Typical hydrodynamic diameters  $d_H$  according to DLS and  $\zeta$ -potential of CDV, PDV, PSV and Au@PSV measured in PBS at pH 7.4. Data represents Z-average and average  $\zeta$ -potential  $\pm$  SD (N = 5).

	$d_H / nm$	$\zeta$ -potential / mV
CDV	$113.0 \pm 1.0$	$-5.9 \pm 0.4$
PDV	$380.9 \pm 6.5$	$-30.1 \pm 0.9$
PSV	$203.9 \pm 6.3$	$-10.6 \pm 0.6$
Au@PSV	$202.9 \pm 6.6$	$-16.4 \pm 0.6$

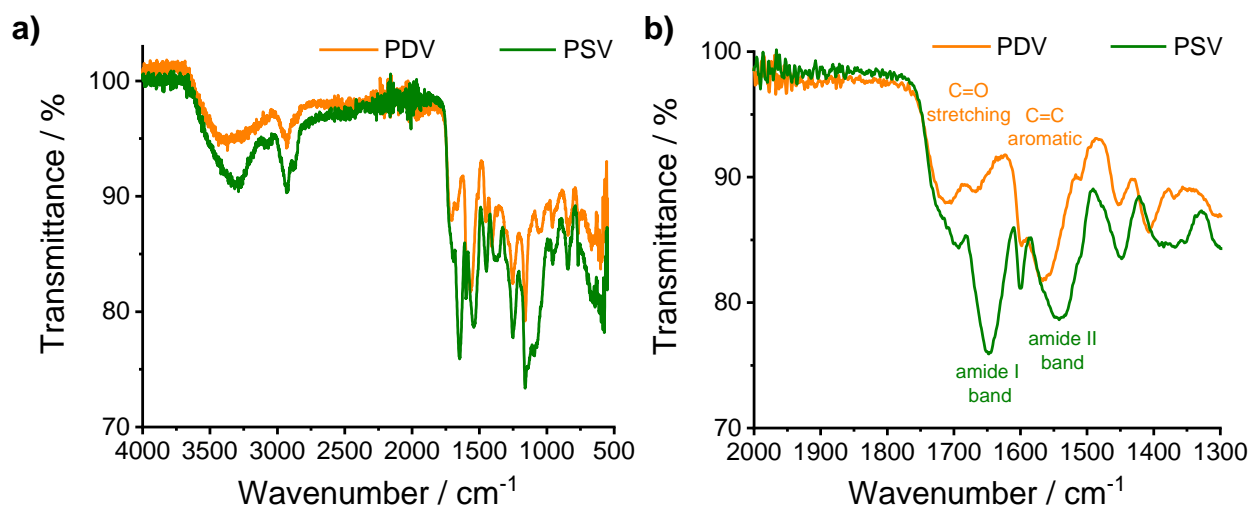


**Figure S1.** a) FT-IR spectra of PDV and PSV. b) Zoomed-in region of amide absorption bands at 1542 cm<sup>-1</sup> and 1648 cm<sup>-1</sup>.<sup>7,8</sup>

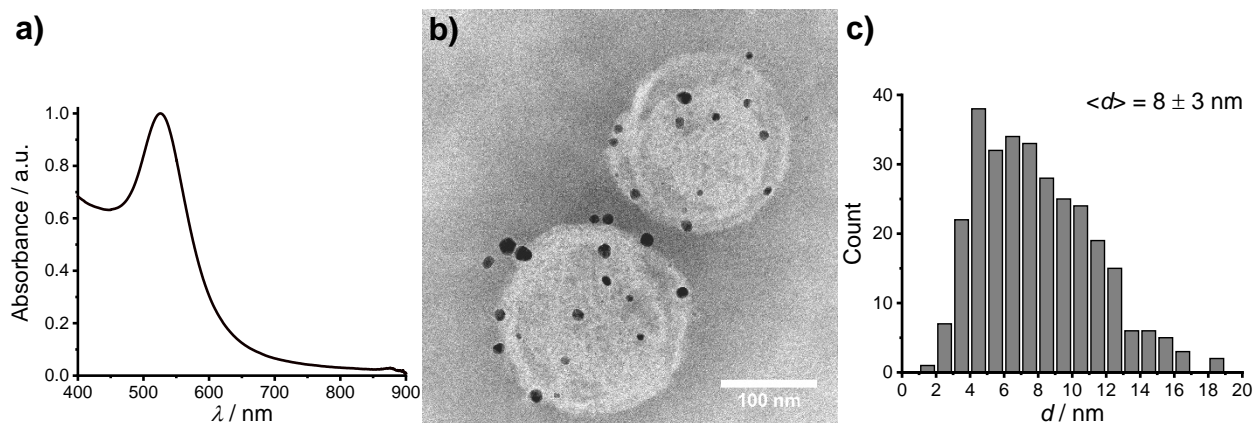


**Figure S2.** a) Absorption spectrum and b) TEM image of Au@PSV prepared without addition of Irgacure-2959. d) Corresponding size histogram of gold nanoparticles ( $N = 150$ ). Notably, the SPR band maximum at  $\lambda_{max} = 526 \text{ nm}$  is redshifted compared to an expected band position slightly below 520 nm for particles with an average size of  $d = 8 \pm 3 \text{ nm}$ .<sup>9,10</sup> This observation is attributed to the polyacrylate matrix of the PSV surrounding the AuNP resulting in an increased refractive index of the nanoparticle environment and a redshifted SPR band.<sup>11–13</sup> Additionally, phosphate buffered saline (20 mM phosphate, 150 mM NaCl, pH 7.4) was used as solvent and the high ionic strength might further increase the refractive index of the surrounding medium and redshift the SPR band.<sup>14,15</sup> Finally, AuNPs exhibit a quite broad distribution of sizes and the fraction of bigger sized particles has a stronger impact to the SPR band position due to their larger extinction coefficient also resulting in a redshifted SPR position.<sup>10,16</sup>

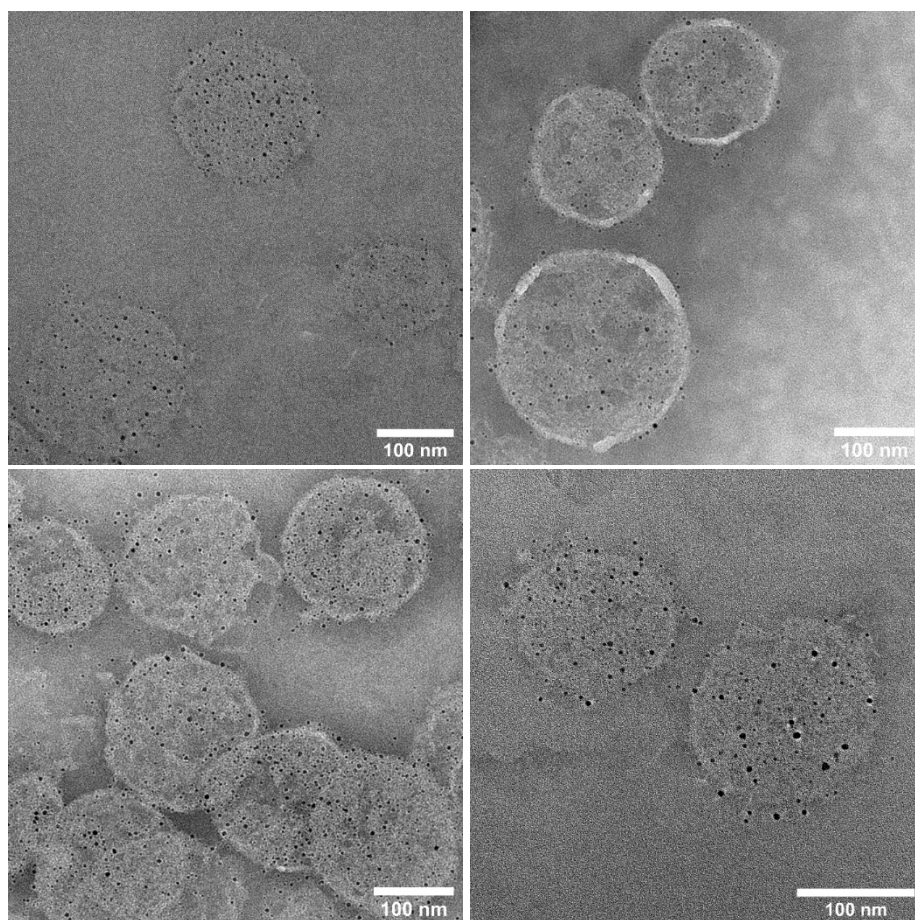


**Figure S3.** TEM images of Au@PSV prepared with addition of 1 equivalent photoinitiator Irgacure-2959.

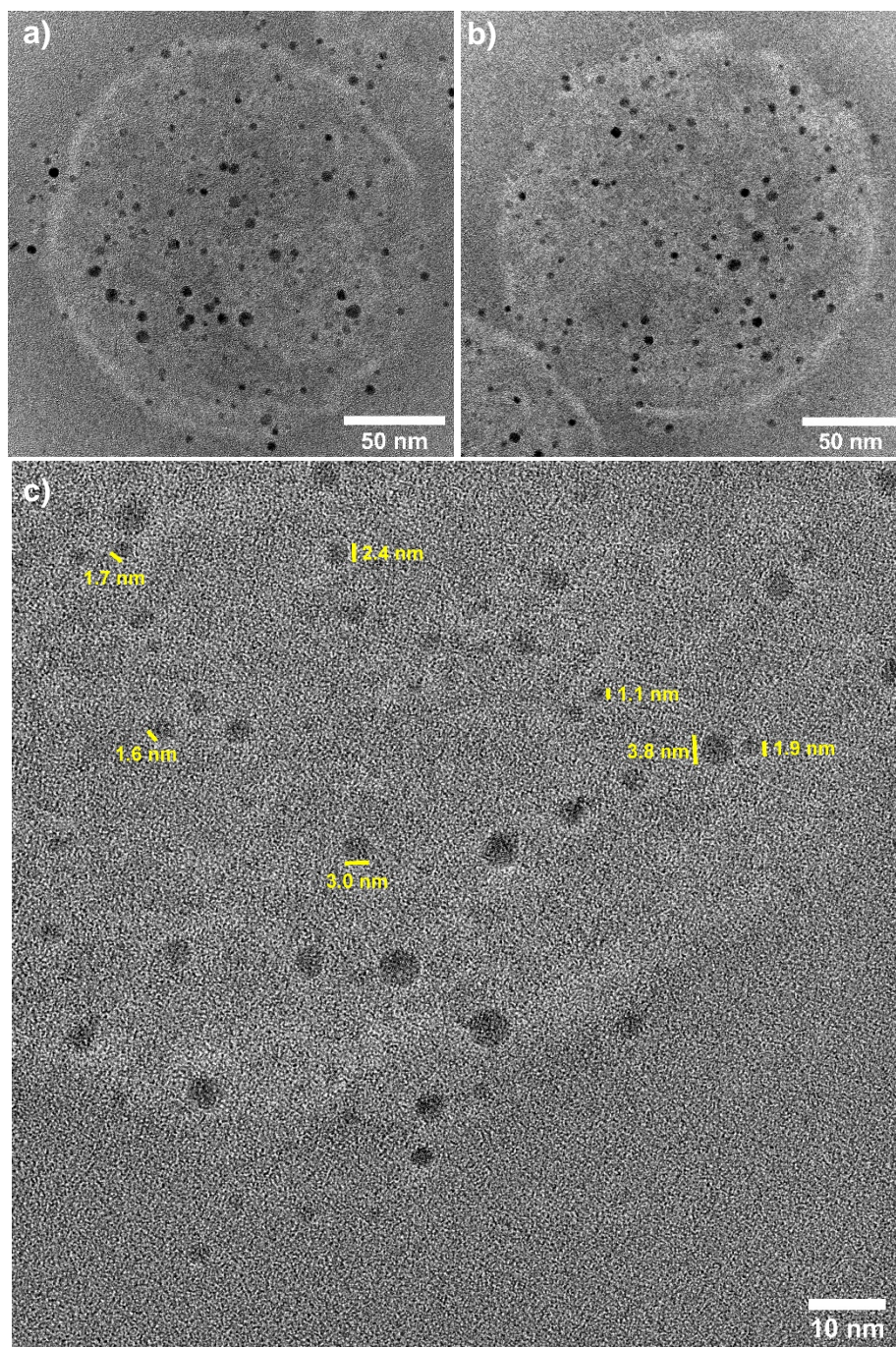


**Figure S4.** a, b) High-magnification TEM images of Au@PSV prepared with addition of 1 equivalent photoinitiator Irgacure-2959. c) HR-TEM image showing a section of an Au@PSV with multiple small gold seeds.

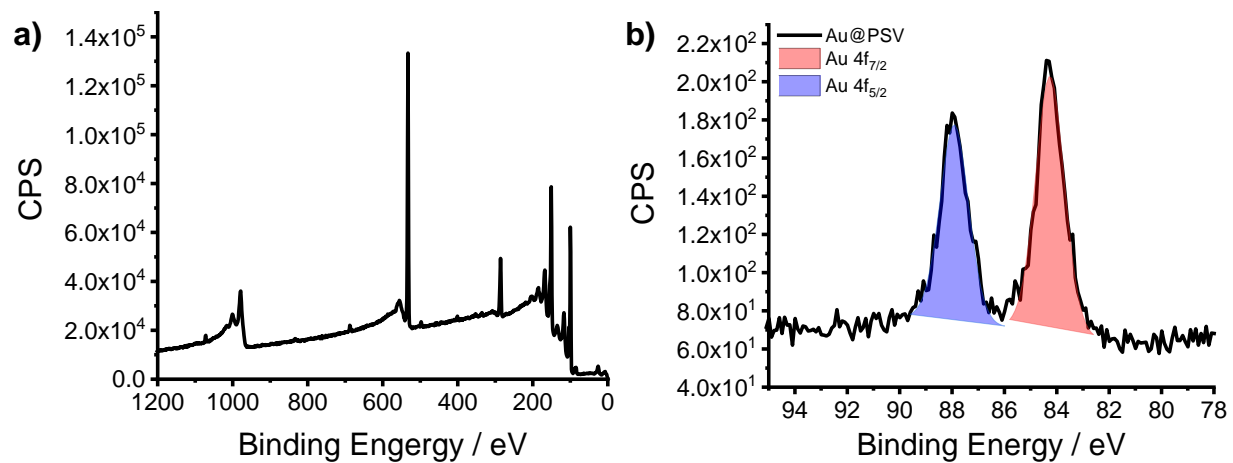


**Figure S5.** XPS spectrum of Au@PSV and zoom-in into Au region with simulated binding energies for Au 4f orbitals.

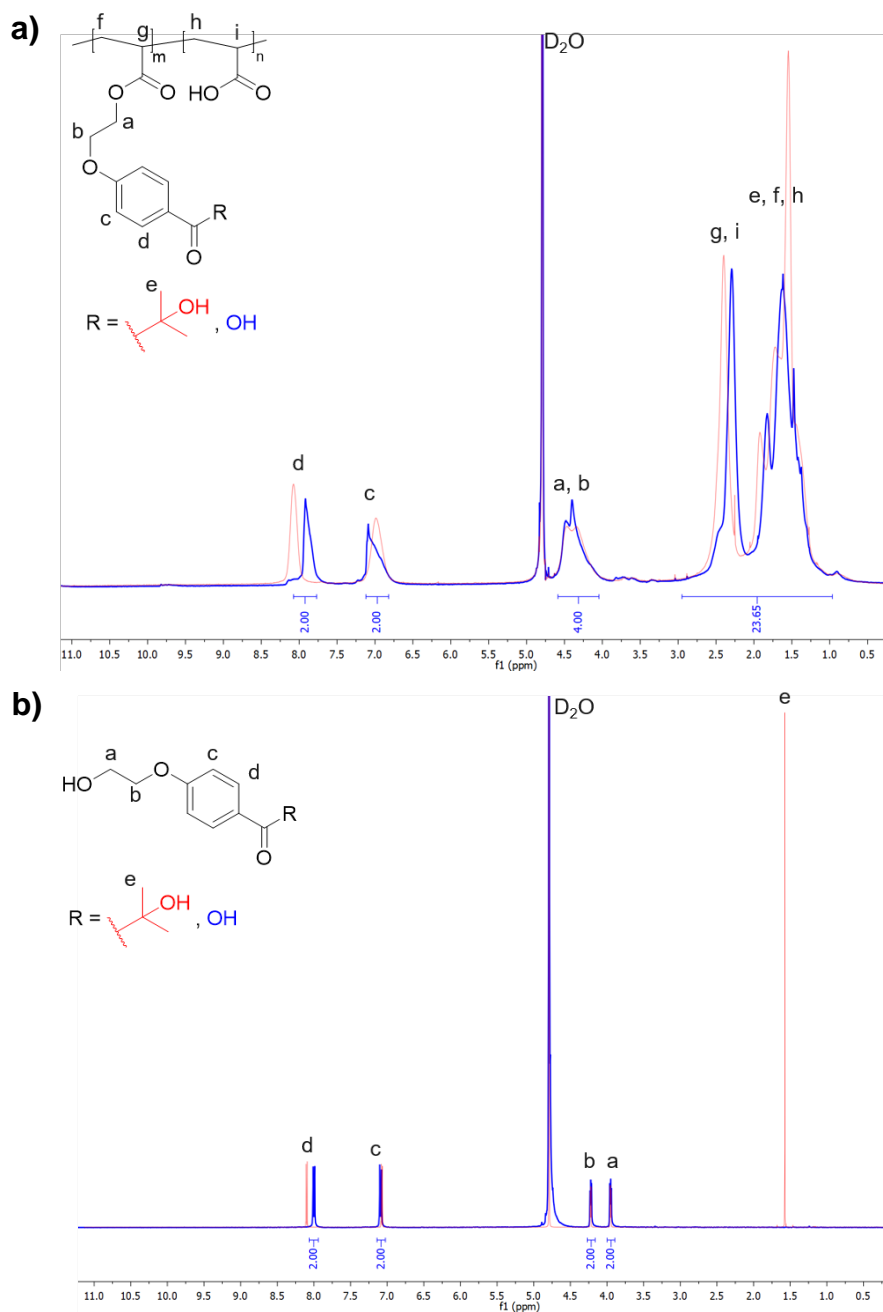


**Figure S6.** a) <sup>1</sup>H-NMR spectrum of Ad-poly(AA-co-HMPA) before (red) and after (blue) UV-light irradiation (30 min) in the presence of Au<sup>3+</sup> (app. 0.3 eq. compared to photoactive HAK units). b) Reference spectra of Irgacure-2959 (red) and 4-(2-hydroxyethoxy)benzoic acid (blue). The shift of aromatic protons (d) and the disappearance of the signal for approximately 6 methyl protons (e) (integration of Ad-poly(AA-co-HMPA) in Fig S16) in comparison with the reference spectra clearly supports the mechanism of Norrish type I photocleavage of HAK-units, followed by conversion of benzoyl radicals into benzoates (Scheme 1b) and is in good agreement with literature reports on the photochemistry of HAK-units by the groups of Scaiano<sup>17,18</sup> and Studer<sup>19</sup>.

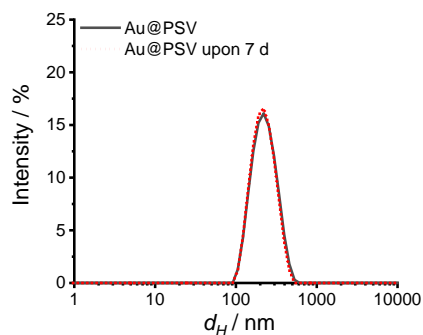


**Figure S7.** Size distributions according to DLS of Au@PSV directly after preparation and after 7 d.

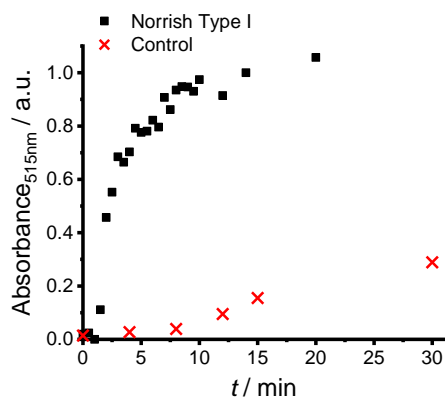


**Figure S8.** Time-dependent evolution of the characteristic SPR band evaluated by the absorbance at  $\lambda = 515$  nm upon photoreduction of gold salts into AuNP. In addition to the synthesis of Au@PSV as described in the Experimental Section (“Norrish Type I”) a control experiment was performed using equal conditions but with PSV<sub>control</sub> lacking the HAK moieties within the polymer shell and without the addition of Irgacure-2959 (“Control”). Samples were irradiated with UVA-lamps ( $\lambda_{max} = 350$  nm).

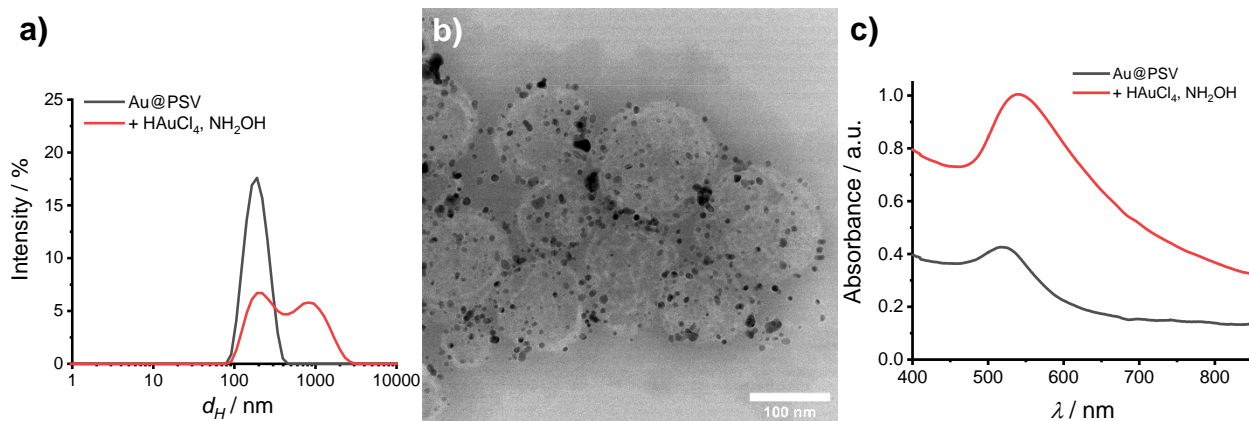


**Figure S9.** Seeded growth of Au@PSV using  $\text{HAuCl}_4$  and  $\text{NH}_2\text{OH}$  in the absence of an additional stabilizer: a) Size distribution according to DLS before (black) and upon seeded growth (red). b) TEM picture of aggregated Au@PSV upon seeded growth showing partial coalescence of Au seeds. c) Absorbance spectra before (black) and upon seeded growth (red).

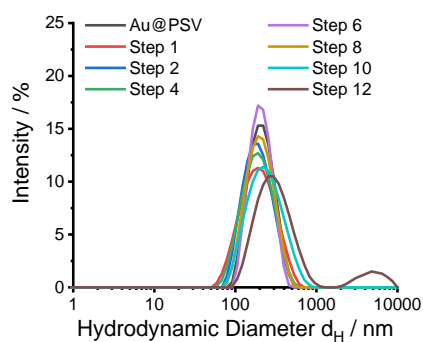


**Figure S10.** Size distributions according to DLS of Au@PSV upon the stepwise addition of  $\text{HAuCl}_4$  and  $\text{NH}_2\text{OH}$  to grow the Au seeds in the presence of 0.1% (w/v) PVP as additional stabilizer.

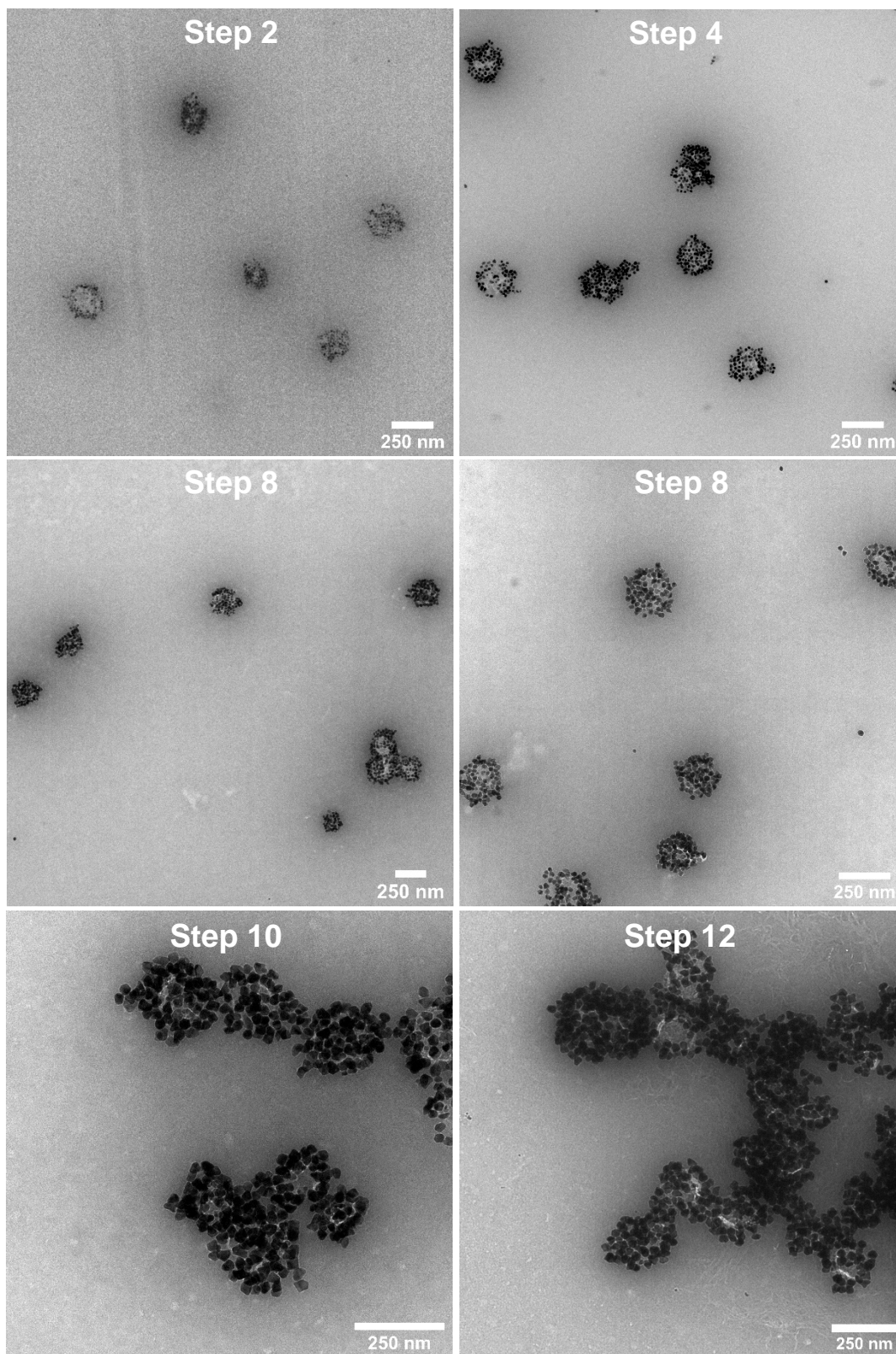


**Figure S11.** TEM pictures of Au@PSV after selected seeded growth steps.

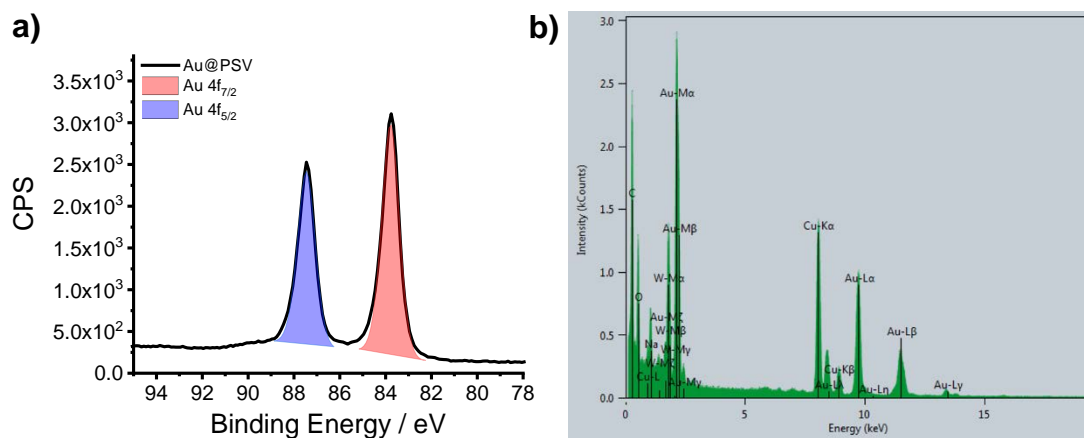


**Figure S12.** a) Au region of the XPS spectrum of Au@PSV upon 8 growth steps with simulated binding energies for Au 4f orbitals. b) EDX spectrum of Au@PSV upon 8 growth steps in correspondence to STEM-EDX image in Figure 3a.

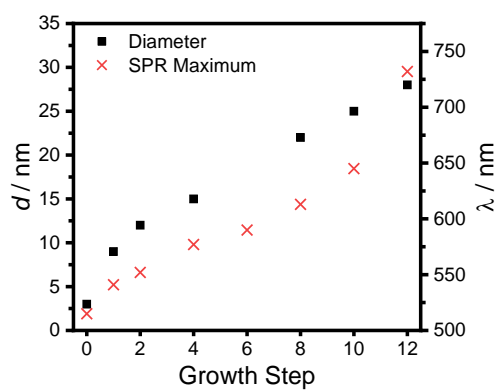


**Figure S13.** Plot of absorption maxima and average AuNP sizes of plasmonic nanocomposites prepared from Au@PSV by a stepwise growth.

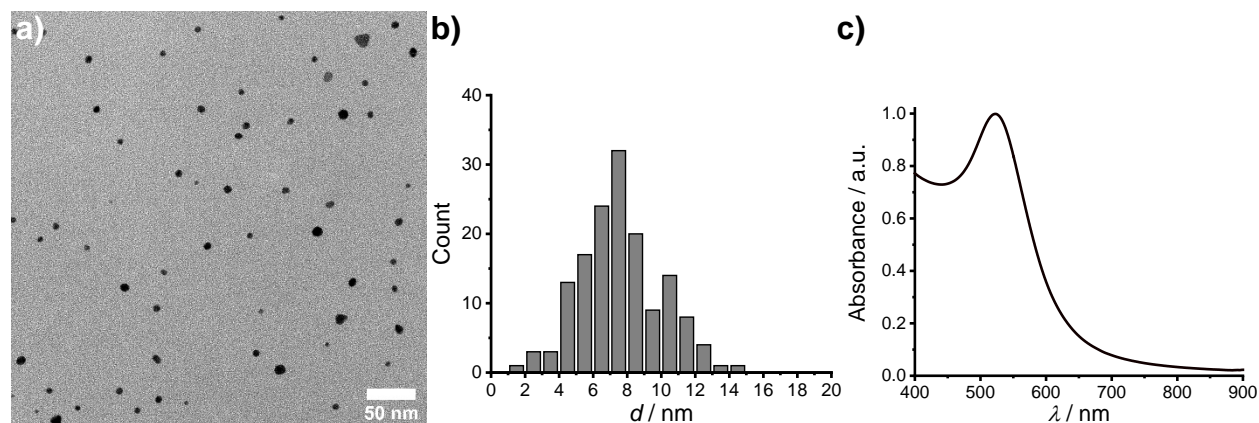


**Figure S14.** a) TEM image, b) size histogram and c) absorption spectrum of reference particles prepared by photochemical reduction of  $\text{HAuCl}_4$  using Ad-poly(AA-*co*-HMPA) without CDV templates.

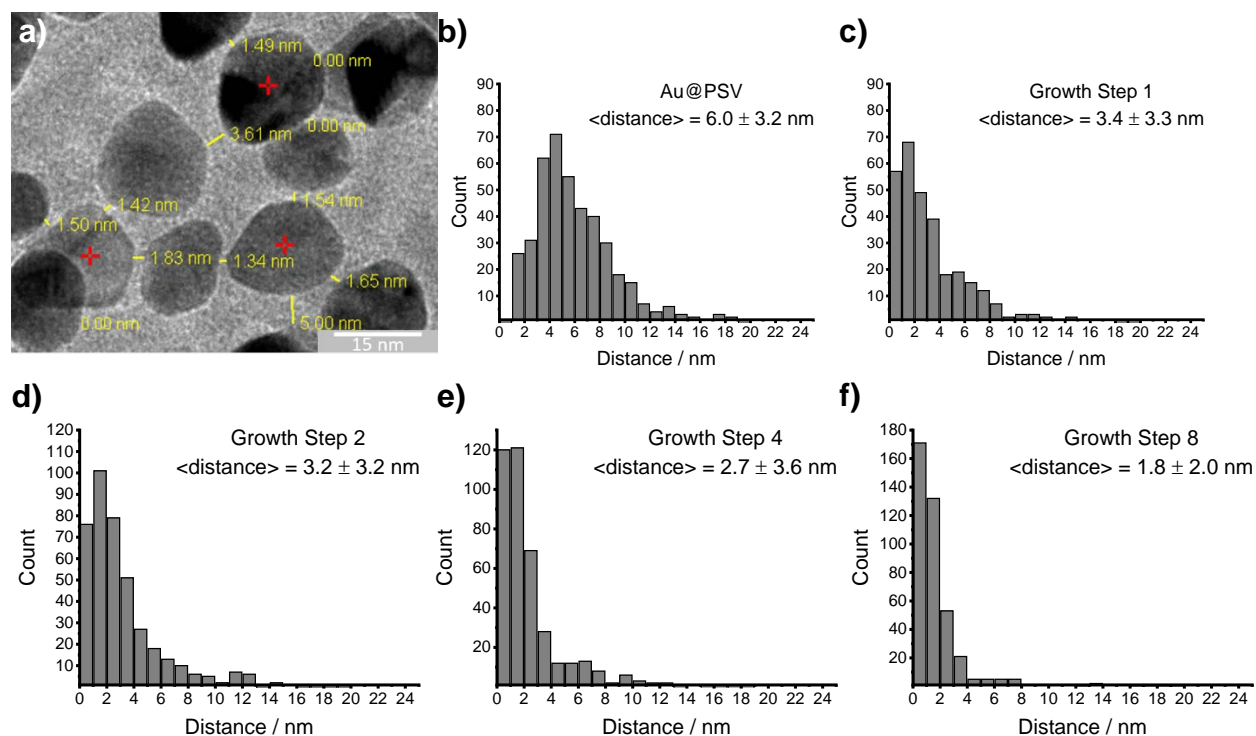


**Figure S15.** Evaluation of interparticle distances from TEM pictures. Edge-to-edge distances were measured for  $N = 100$  particles and for every particle the distance to the four closest neighboring particles was evaluated. Notably, these distances represent a rough estimation of interparticle distances as the distances will decrease upon drying of the samples for TEM preparation and therefore apparent distances will slightly underestimate AuNP distances in solution. Additionally, TEM images represent a 2D projection of the spherical Au@PSV and overlapping particles were counted with a distance of 0.00 nm. Therefore, the measured distances primarily must be interpreted in regard to the measured redshift of the SPR band and in combination with the

literature discussed in the article main text. a) Exemplary TEM image illustrating the measurement of distances to the neighboring particles for three particles (marked with a red cross). b-f) Histograms of the edge-to-edge interparticle distances for selected growth steps. Distances for more than 8 growth steps have not been evaluated, because of the clustering of vesicular structures resulting in an overlap of almost all particles in the TEM pictures.

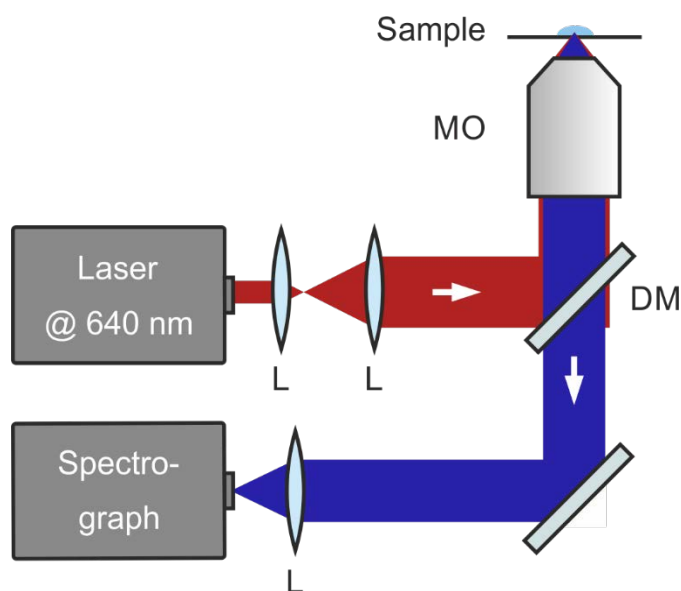


**Figure S16.** Schematic of the custom-built setup for the measurement of spontaneous Raman spectra with microscope objective (MO), lens (L) and dichroic mirror (DM).

**Table S2.** Assignment of characteristic Raman bands in SERS spectra of Ad-RhoB using Au@PSV upon 8 growth steps as a SERS substrate.<sup>20-23</sup> (X = xanthene ring, A = adamantane, E = NEt)

SERS / $\text{cm}^{-1}$	Assignment
1629	C <sub>X</sub> -C <sub>X</sub> stretching
1510, 1496	C <sub>X</sub> -C <sub>X</sub> stretching, C <sub>E</sub> -N stretching
1346	C <sub>X</sub> -C <sub>X</sub> stretching
1269	C-O-C stretching
1193, 1075	C <sub>X</sub> -C <sub>X</sub> stretching, C <sub>E</sub> -H bending
743	C <sub>A</sub> -C <sub>A</sub> stretching
630, 670	C <sub>X</sub> -C <sub>X</sub> -C <sub>X</sub> bending

## <sup>1</sup>H-NMR and GPC Trace of copolymers

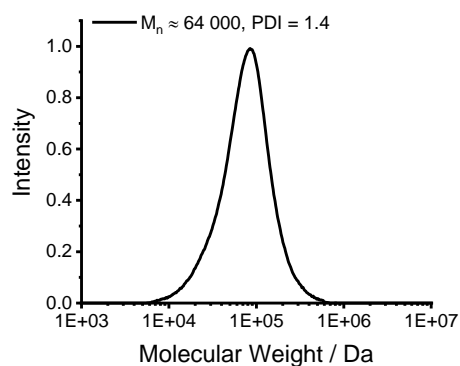


**Figure S17.** GPC (SEC) trace of adamantyl terminated poly(*tert*-butyl acrylate-*co*-2-(4-(2-hydroxy-2-methylpropanoyl)phenoxy)ethyl acrylate) (Ad-poly(*t*BuA-*co*-HMPA)).

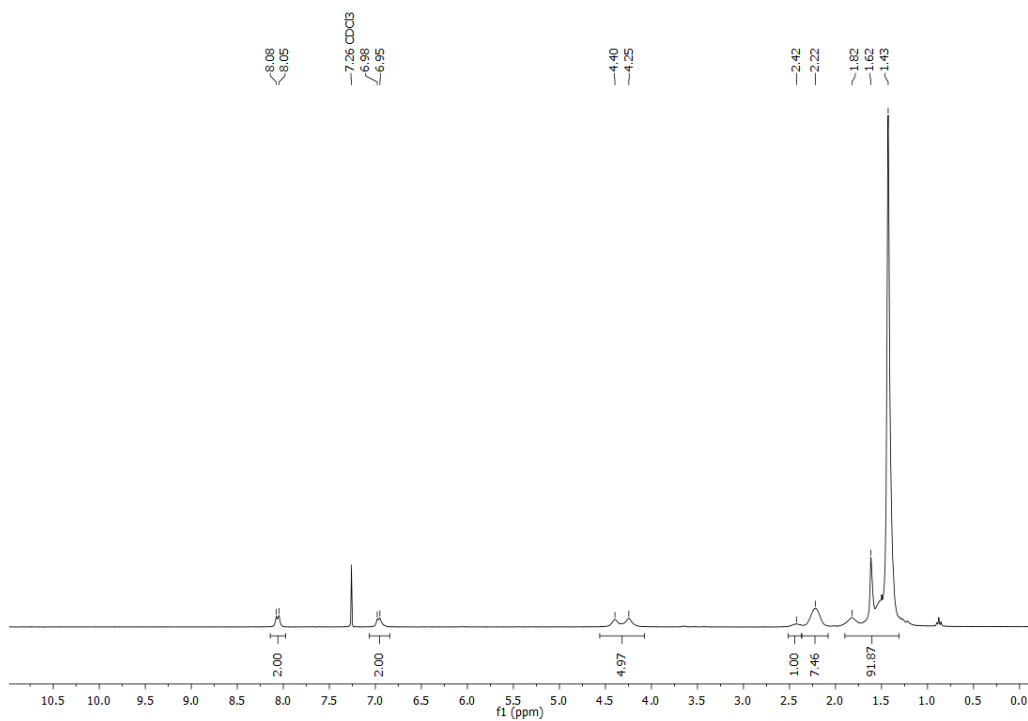


**Figure S18:** <sup>1</sup>H-NMR spectrum of adamantyl terminated poly(*tert*-butyl acrylate-*co*-2-(4-(2-hydroxy-2-methylpropanoyl)phenoxy)ethyl acrylate) (Ad-poly(*t*BuA-*co*-HMPA **4**)).

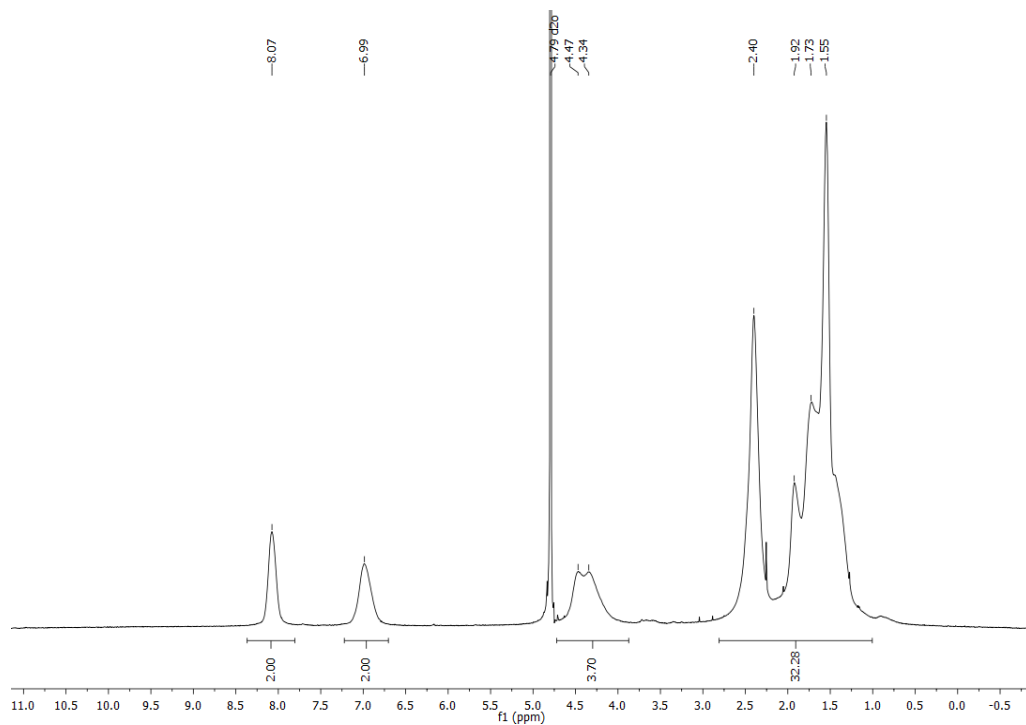


**Figure S19:** <sup>1</sup>H-NMR spectrum of adamantyl terminated poly(acrylic acid-*co*-2-(4-(2-Hydroxy-2-methylpropanoyl)phenoxy)ethyl acrylate) (Ad-poly(AA-*co*-HMPA 5)).

## References

- 1 A. Samanta, M. Tesch, U. Keller, J. Klingauf, A. Studer and B. J. Ravoo, *J. Am. Chem. Soc.*, 2015, **137**, 1967–1971.
- 2 F. Mäsing, X. Wang, H. Nüsse, J. Klingauf and A. Studer, *Chem. Eur. J.*, 2017, **23**, 6014–6018.
- 3 B. J. Ravoo and R. Darcy, *Angew. Chem. Int. Ed.*, 2000, **39**, 4324–4326.
- 4 P. Falvey, C. W. Lim, R. Darcy, T. Revermann, U. Karst, M. Giesbers, A. T. M. Marcelis, A. Lazar, A. W. Coleman, D. N. Reinhoudt and B. J. Ravoo, *Chem. Eur. J.*, 2005, **11**, 1171–1180.
- 5 U. Kauscher, M. C. A. Stuart, P. Drücker, H. J. Galla and B. J. Ravoo, *Langmuir*, 2013, **29**, 7377–7383.
- 6 Y. Gao, W. Yao, J. Sun, H. Zhang, Z. Wang, L. Wang, D. Yang, L. Zhang and H. Yang, *J. Mater. Chem. A*, 2015, **3**, 10738–10746.
- 7 S.-M. Lee, H. Chen, C. M. Dettmer, T. V. O’Halloran and S. T. Nguyen, *J. Am. Chem. Soc.*, 2007, **129**, 15096–15097.
- 8 A. Barth, *Biochim. Biophys. Acta*, 2007, **1767**, 1073–1101.
- 9 S. Link and M. A. El-Sayed, *J. Phys. Chem. B*, 1999, **103**, 4212–4217.
- 10 P. K. Jain, K. S. Lee, I. H. El-Sayed and M. A. El-Sayed, *J. Phys. Chem. B*, 2006, **110**, 7238–7248.
- 11 H. Jans, K. Jans, L. Lagae, G. Borghs, G. Maes and Q. Huo, *Nanotechnology*, 2010, **21**, 455702.
- 12 X. Li, L. Jiang, Q. Zhan, J. Qian and S. He, *Colloids Surfaces A Physicochem. Eng. Asp.*, 2009, **332**, 172–179.
- 13 G. Schneider and G. Decher, *Langmuir*, 2008, **24**, 1778–1789.
- 14 A. Dorris, S. Rucareanu, L. Reven, C. J. Barrett and R. Bruce Lennox, *Langmuir*, 2008, **24**, 2532–2538.
- 15 A. Vincenzo, P. Roberto, F. Marco, M. M. Onofrio and I. Maria Antonia, *J. Phys. Condens. Matter*, 2017, **29**, 203002.

- 16 X. Liu, M. Atwater, J. Wang and Q. Huo, *Colloids Surfaces B Biointerfaces*, 2007, **58**, 3–7.
- 17 M. L. Marin, K. L. McGilvray and J. C. Scaiano, *J. Am. Chem. Soc.*, 2008, **130**, 16572–16584.
- 18 J. C. Scaiano, K. G. Stamplecoskie and G. L. Hallett-Tapley, *Chem. Commun.*, 2012, **48**, 4798–4808.
- 19 F. Mäsing, A. Mardyukov, C. Doerenkamp, H. Eckert, U. Malkus, H. Nüsse, J. Klingauf and A. Studer, *Angew. Chem. Int. Ed.*, 2015, **54**, 12612–12617.
- 20 P. Hildebrandt and M. Stockburger, *J. Phys. Chem.*, 1984, **88**, 5935–5944.
- 21 C. H. Sun, M. L. Wang, Q. Feng, W. Liu and C. X. Xu, *Russ. J. Phys. Chem. A*, 2015, **89**, 291–296.
- 22 J. Filik, J. N. Harvey, N. L. Allan, P. W. May, J. E. P. Dahl, S. Liu and R. M. K. Carlson, *Spectrochim. Acta A*, 2006, **64**, 681–692.
- 23 H. Watanabe, N. Hayazawa, Y. Inouye and S. Kawata, *J. Phys. Chem. B*, 2005, **109**, 5012–5020.